

Blue-Green Emissive Cationic Iridium(III) Complexes Using Partially Saturated Strongly-Donating Guanidyl-pyridine/pyrazine Ancillary Ligands

Kamrul Hasan,^a Amlan K Pal,^a Thomas Auvray,^a Eli Zysman-Colman^{*b} and Garry S Hanan^{*a}

^aDépartement de Chimie, Université de Montréal, 2900 Edouard-Montpetit, Montréal, Québec H3T-1J4, Canada. E-mail: garry.hanan@umontreal.ca; Fax: +1-514 343-2468; Tel: +1-514 343-7056

^bOrganic Semiconductor Centre, EaStCHEM School of Chemistry, University of St Andrews, St Andrews, Fife, UK, KY16 9ST, Fax: +44-1334 463808; Tel: +44-1334 463826; E-mail: eli.zysman-colman@st-andrews.ac.uk;
URL: <http://www.zysman-colman.com>

SUPPORTING INFORMATION

Table of contents

	Pages
Materials, method and instrumentation	S2-S4
Synthetic details	S5-S7
¹ H, ¹⁹ F and ¹³ C NMR spectrum of individual compounds and complexes	S8-S13
X-ray diffraction studies	S13-S16
UV-vis spectra and molar absorptivity data of complexes	S17
Cyclic voltammograms and electrochemical data of complexes	S18-S19
Computational output	S20-S31
References	S32-S33

Materials, method and instrumentation:

General Synthetic Procedures. Commercial chemicals were used as supplied. All reactions were performed using standard Schlenk techniques under inert (N_2) atmosphere with freshly distilled anhydrous solvents obtained from a Pure MBRAUN (MB-SPS) purification system except where specifically mentioned. Flash column chromatography was performed using silica gel (Silia-P from Silicycle, 60 Å, 40-63 µm). Analytical thin layer chromatography (TLC) was performed with silica plates with aluminum backings (250 µm with indicator F-254). Compounds were visualized under UV light. 1H , ^{19}F and ^{13}C NMR spectra were recorded on a Brucker Avance 400 spectrometer at 400 MHz, 376 MHz and 100 MHz, respectively. The following abbreviations have been used for multiplicity assignments: “s” for singlet, “d” for doublet, “t” for triplet, “m” for multiplet and “br” for broad. Deuterated chloroform ($CDCl_3$), deuterated acetone ($CD_3)_2CO$ and deuterated acetonitrile (CD_3CN) were used as the solvent of record. Chemical shifts are reported in part per million (ppm) relative to residual solvent protons (1.96 ppm for CD_3CN , 7.26 ppm for $CDCl_3$ and 2.07 for $(CD_3)_2CO$) and the carbon resonance (0.73 and 118.69 ppm for CD_3CN , 77.00 ppm for $CDCl_3$ and 29.34 and 205.64 for $(CD_3)_2CO$) of the solvent. Melting points (Mp’s) were recorded using open-ended capillaries on a Meltemp melting point apparatus and are uncorrected. High resolution mass spectra were recorded on a quadrupole time-of-flight (ESI-Q-TOF), model MICROTOF II from Bruker in positive electrospray ionization mode at the Université de Montréal. 1,3,4,6,7,8-Hexahydro-2H-pyrimido[1,2-*a*]pyrimidine (H-hpp), 2-bromopyridine, 2-chloropyrazine, (±) BINAP, $Pd(OAc)_2$, *t*-BuOK were purchased from Aldrich and used as received. The corresponding iridium(III) dimers, $[(C^N)_2Ir(Cl)]_2$ were prepared

according to the literature, where C^N is 2-phenylpyridinato or 2-(2,4-difluorophenyl)-5-methylpyridinato.¹

Photophysical measurements. All samples were prepared in HPLC grade acetonitrile (ACN) with varying concentrations on the order of μM . Absorption spectra were recorded at RT using a Cary 500i double beam spectrophotometer. Molar absorptivity determination was verified by linear least-squares fit of values obtained from at least three independent solutions at varying concentrations with absorbance ranging from 6.88×10^{-1} to $3.19 \times 10^2 \mu\text{M}$.

The sample solutions for the emission spectra were prepared in Ar-degassed dry ACN. Emission spectra were recorded at room temperature using a Cary Eclipse 300 fluorimeter or a Perkin Elmer LS55 fluorimeter. The samples were excited at the absorption maxima of the dominant low-energy ¹MLCT band as indicated in Table S3. Excited state lifetimes were measured with an Edinburgh Instruments Mini Tau lifetime fluorimeter with an EPL 405 laser (exciting at 405 nm). Emission quantum yields were determined using the optically dilute method.² A stock solution with absorbance of ca. 0.5 was prepared and then four dilutions were prepared with dilution factors of 40, 20, 13.3 and 10 to obtain solutions with absorbances of ca. 0.013, 0.025, 0.038 and 0.05, respectively. The Beer-Lambert law was found to be linear at the concentrations of the solutions. The emission spectra were then measured after the solutions were rigorously degassed with solvent-saturated argon gas (Ar) for 20 minutes prior to spectrum acquisition using septa-sealed quartz cells from Starna. For each sample, linearity between absorption and emission intensity was verified through linear regression analysis and additional measurements were acquired until the Pearson regression factor (R^2) for the linear fit of the data set surpassed 0.9. Individual relative quantum yield values were calculated for each solution and the values

reported represent the slope value. The equation $\Phi_s = \Phi_r(A_r/A_s)(I_s/I_r)(n_s/n_r)^2$ was used to calculate the relative quantum yield of each of the sample, where Φ_r is the absolute quantum yield of the reference, n is the refractive index of the solvent, A is the absorbance at the excitation wavelength, and I is the integrated area under the corrected emission curve. The subscripts s and r refer to the sample and reference, respectively. A solution of quinine sulfate in ACN ($\Phi_r = 0.54$) was used as the external reference.³

Electrochemistry measurements. Cyclic voltammetry (CV) measurements were performed in argon-purged purified HPLC grade acetonitrile at room temperature with a BAS CV50W multipurpose equipment interfaced to a PC or a Biologic SP-50 potentiostat. Solutions for cyclic voltammetry were prepared in ACN and degassed with ACN-saturated argon bubbling for about 20 min prior to scanning. Tetra(*n*-butyl)ammonium hexafluorophosphate (TBAPF₆; ca. 0.1 M in ACN) was used as the supporting electrolyte. A non-aqueous Ag/Ag⁺ electrode (silver wire in a solution of 0.1 M AgNO₃ in ACN) was used as the pseudoreference electrode; a glassy-carbon electrode was used for the working electrode and a Pt electrode was used as the counter electrode. The redox potentials are reported relative to a standard calomel electrode (SCE) electrode with a ferrocenium/ferrocene (Fc⁺/Fc) redox couple as an internal reference (0.38 V vs SCE).⁴

Synthetic details:

1-(Pyridin-2-yl)-2,3,4,6,7,8- hexahydro-1*H*-pyrimido[1,2-*a*]pyrimidine (Guanidyl-pyridine (gpy), **L1**): The synthesis was carried out according to our recently reported protocol.⁵

Yield: 95%. ¹H NMR (400 MHz, Chloroform-*d*) δ (ppm): 8.25 (ddd, *J* = 5.0, 1.9, 0.8 Hz, 1H), 7.69 – 7.66 (m, 1H), 7.50 – 7.45 (m, 1H), 6.78 (ddd, *J* = 7.1, 5.0, 1.0 Hz, 1H), 3.92 – 3.87 (m, 1H), 3.45 – 3.40 (m, 1H), 3.24 (t, *J* = 6.0 Hz, 1H), 3.20 (t, *J* = 6.4 Hz, 1H), 2.07 – 2.00 (m, 1H), 1.93 – 1.86 (m, 1H). ¹³C NMR (101 MHz, CDCl₃) δ (ppm): 156.93, 150.13, 147.38, 136.10,

118.97, 116.97, 49.12, 48.90, 44.23, 43.87, 24.03, 23.04. The ^1H and ^{13}C NMR are in good agreement with previously reported result.⁵

1-(Pyrazin-2-yl)-2,3,4,6,7,8-hexahydro-1H-pyrimido[1,2- α]- pyrimidine (Guanidyl-pyrazine (gpz), L2): The synthesis was carried out according to our recently reported protocol.⁵ **Yield:** 82 %. ^1H NMR (400 MHz, Chloroform- d) δ (ppm): 9.10 – 9.08 (m, 1H), 8.14 (dd, J = 2.8, 1.5 Hz, 1H), 7.96 (d, J = 2.7 Hz, 1H), 3.87 – 3.83 (m, 2H), 3.46 – 3.42 (m, 2H), 3.27 (t, J = 6.0 Hz, 2H), 3.23 (t, J = 6.3 Hz, 2H), 2.11 – 2.03 (m, 2H), 1.92 (dt, J = 11.7, 5.9 Hz, 2H). ^{13}C NMR (101 MHz, CDCl₃) δ (ppm): 207.35, 153.42, 149.05, 142.42, 141.03, 135.58, 49.01, 48.78, 44.05, 43.18, 31.33, 23.87, 22.91. The ^1H and ^{13}C NMR are in good agreement with previously reported result.⁵

General procedure for the synthesis of $[(C^N)_2\text{Ir}(N^N)]\text{PF}_6$ complexes. Iridium dimer (0.07 mmol, 1.0 equiv.) and N^N ligand (gpy or gpz) (0.15 mmol, 2.10 equiv.) were solubilized with 20 mL of DCM/MeOH (50:50). The mixture was degassed by multiple vacuum and N₂ purging cycles. The suspension was heated at 50 °C for 19 h. The reaction mixture was cooled to room temperature and evaporated to dryness. The resulted solid was dissolved in minimum amount of MeOH and a solution of NH₄PF₆ (10 equiv., 1.0 g / 10 mL) was added drop by drop to the methanolic solution to cause the precipitation of a solid. The suspension was cooled to 0 °C for 1 h, filtered and the resulting solid was washed with cold water. The crude solid was purified by flash chromatography on silica gel using DCM to DCM/Acetone (9/1).

$[(\text{ppy})_2\text{Ir}(\text{gpy})]\text{PF}_6$, **1.** Light yellow solid. **Yield:** 90%. Mp: 191–192 °C. R_f: 0.25 (DCM/acetone (5%) on silica. ^1H NMR (400 MHz, Acetone- d_6) δ (ppm): 8.71 (dd, J = 5.9, 1.4 Hz, 1H), 8.46 (dd, J = 5.9, 1.3 Hz, 1H), 8.29 – 8.25 (m, 1H), 8.22 (dd, J = 8.2, 1.3 Hz, 1H), 8.07 – 7.99 (m,

3H), 7.85 (dd, J = 7.6, 1.4 Hz, 1H), 7.78 – 7.70 (m, 2H), 7.59 – 7.55 (m, 1H), 7.37 (ddt, J = 9.0, 7.1, 3.5 Hz, 2H), 7.02 (ddd, J = 7.1, 5.7, 1.2 Hz, 1H), 6.90 (tdd, J = 7.5, 6.2, 1.3 Hz, 2H), 6.75 (qd, J = 7.5, 1.4 Hz, 2H), 6.29 (dd, J = 7.5, 1.3 Hz, 1H), 6.19 (dd, J = 7.6, 1.2 Hz, 1H), 4.11 (dt, J = 14.1, 4.7 Hz, 1H), 3.54 (tdd, J = 12.8, 8.6, 3.7 Hz, 2H), 3.38 (dt, J = 12.0, 8.2 Hz, 1H), 3.34 – 3.22 (m, 2H), 3.16 (dt, J = 11.5, 5.3 Hz, 1H), 3.09 – 3.01 (m, 1H), 2.44 (ddt, J = 11.8, 8.0, 4.4 Hz, 1H), 2.33 (td, J = 10.5, 9.2, 5.0 Hz, 1H), 1.65 – 1.56 (m, 1H), 1.12 (dt, J = 13.4, 3.9 Hz, 1H). ^{13}C NMR (101 MHz, Acetone- d_6) δ (ppm): 168.71, 168.66, 155.25, 153.67, 153.45, 151.33, 150.74, 150.69, 149.87, 144.99, 144.86, 140.70, 138.64, 138.41, 132.36, 129.89, 125.39, 124.34, 123.09, 122.79, 122.03, 121.90, 120.18, 119.66, 118.00, 48.96, 48.79, 48.59, 46.88, 23.15, 22.99. HR-MS (ES-Q-TOF): $[\text{M-PF}_6]^+$ ($\text{C}_{34}\text{H}_{32}\text{N}_6\text{Ir}^+$) Calculated: 717.2314; Experimental: 717.2313.

$[(\text{dFMeppy})_2\text{Ir}(\text{gpy})]\text{PF}_6$, **2**. Light yellow solid. **Yield:** 82%. Mp: 184–185 °C. R_f : 0.28 (DCM/acetone (5%) on silica. ^1H NMR (400 MHz, Acetone- d_6) δ (ppm): 8.56 (s, 1H), 8.44 (d, J = 2.0 Hz, 1H), 8.35 (dd, J = 8.4, 1.7 Hz, 1H), 8.30 – 8.24 (m, 1H), 8.11 – 8.05 (m, 1H), 7.99 (t, J = 7.5 Hz, 2H), 7.78 (d, J = 8.4 Hz, 1H), 7.59 – 7.52 (m, 1H), 7.09 (t, J = 6.6 Hz, 1H), 6.59 (ddt, J = 11.9, 9.2, 2.2 Hz, 2H), 5.77 (dd, J = 8.6, 2.4 Hz, 1H), 5.60 (dd, J = 8.8, 2.4 Hz, 1H), 4.24 – 4.16 (m, 1H), 3.62 – 3.53 (m, 2H), 3.47 – 3.37 (m, 2H), 3.32 (dt, J = 10.5, 5.8 Hz, 1H), 3.21 (dt, J = 11.5, 4.9 Hz, 1H), 2.49 (s, 1H), 2.44 (s, 3H), 2.41 (s, 3H), 2.33 (s, 1H), 1.75 (s, 1H), 1.24 – 1.11 (m, 1H). ^{19}F NMR (376 MHz, Acetonitrile- d_3) δ (ppm): -73.17, -75.03, -111.02 – -111.38 (m), -111.41 (d, J = 9.1 Hz), -111.99 (t, J = 11.4 Hz), -113.27 – -113.81 (m). ^{13}C NMR (101 MHz, Acetone- d_6) δ (ppm): 164.32, 162.08, 157.68, 154.98, 154.72, 153.63, 151.51, 150.63, 150.04, 141.27, 140.44, 140.29, 134.04, 133.78, 128.77, 123.58, 123.39, 122.85, 122.66, 122.53, 118.41, 114.34, 114.17, 98.23, 97.95, 97.70, 48.97, 48.85, 48.54, 47.16, 23.11, 17.76, 17.40. HR-MS (ES-Q-TOF): $[\text{M-PF}_6]^+$ ($\text{C}_{36}\text{H}_{32}\text{N}_6\text{IrF}_4^+$) Calculated: 817.2250; Experimental: 817.2253.

[(ppy)₂Ir(gpz)]PF₆, **3**. Light red solid. **Yield:** 80%. Mp: 238 °C. R_f: 0.32 (DCM/acetone (5%) on silica. ¹H NMR (400 MHz, Acetonitrile-*d*₃) δ 8.76 (d, *J* = 1.0 Hz, 1H), 8.55 – 8.51 (m, 1H), 8.28 (dd, *J* = 5.8, 0.7 Hz, 1H), 8.15 (d, *J* = 7.9 Hz, 1H), 8.09 (d, *J* = 7.9 Hz, 1H), 8.01 (d, *J* = 3.3 Hz, 1H), 8.00 – 7.94 (m, 2H), 7.80 (dd, *J* = 7.8, 1.0 Hz, 1H), 7.71 (dd, *J* = 7.8, 1.1 Hz, 1H), 7.42 (dd, *J* = 3.3, 1.0 Hz, 1H), 7.30 (ddd, *J* = 7.4, 5.9, 1.4 Hz, 1H), 7.24 (ddd, *J* = 7.3, 5.9, 1.5 Hz, 1H), 6.99 – 6.90 (m, 2H), 6.79 (tt, *J* = 7.5, 1.3 Hz, 2H), 6.24 – 6.20 (m, 1H), 6.15 – 6.10 (m, 1H), 3.95 (ddd, *J* = 14.2, 5.9, 3.5 Hz, 1H), 3.49 – 3.37 (m, 2H), 3.30 – 3.24 (m, 1H), 3.23 – 3.15 (m, 1H), 3.14 – 3.01 (m, 2H), 2.93 – 2.85 (m, 1H), 2.34 (tdt, *J* = 11.6, 8.1, 4.1 Hz, 1H), 2.26 – 2.19 (m, 1H), 1.60 – 1.50 (m, 1H), 1.08 (ddq, *J* = 13.1, 5.9, 3.4 Hz, 1H). ¹³C NMR (101 MHz, Acetonitrile-*d*₃) δ (ppm): 168.31, 168.07, 152.71, 152.51, 151.10, 150.97, 150.61, 150.25, 145.13, 144.72, 142.31, 141.42, 140.99, 138.87, 138.61, 132.33, 132.17, 130.11, 130.02, 125.45, 124.43, 123.30, 122.92, 122.34, 122.26, 120.41, 119.84, 48.89, 48.70, 48.03, 46.96, 22.99, 22.81. HR-MS (ES-Q-TOF): [M-PF₆]⁺ (C₃₃H₃₁N₇Ir⁺) Calculated: 718.2266; Experimental: 718.2245.

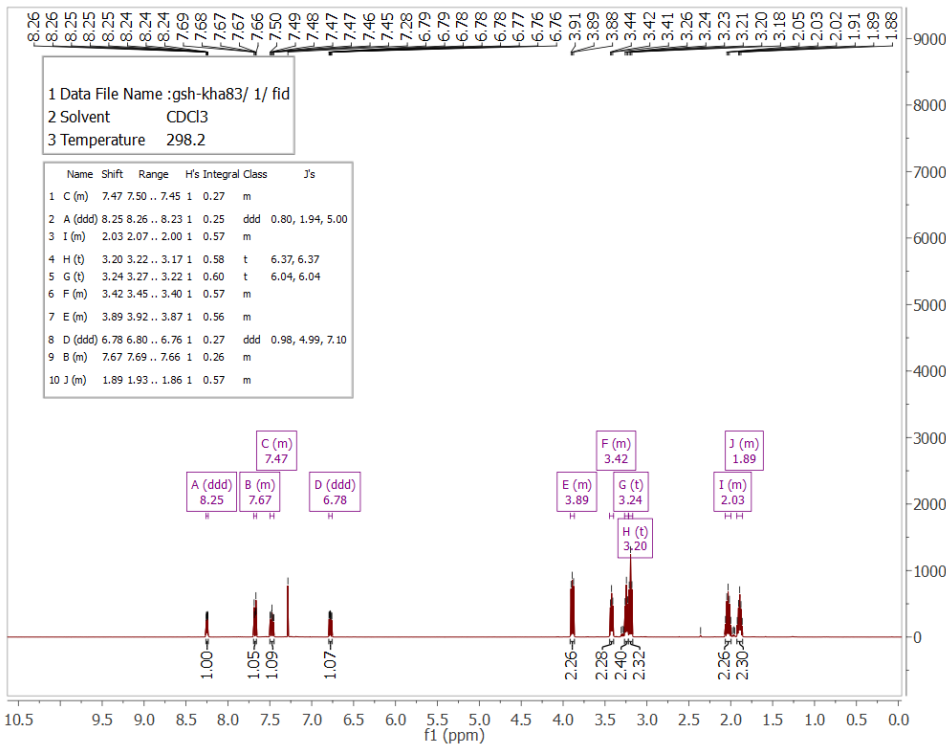


Figure S1. ^1H NMR spectrum of Guanidyl-pyridine, gpy in CDCl_3

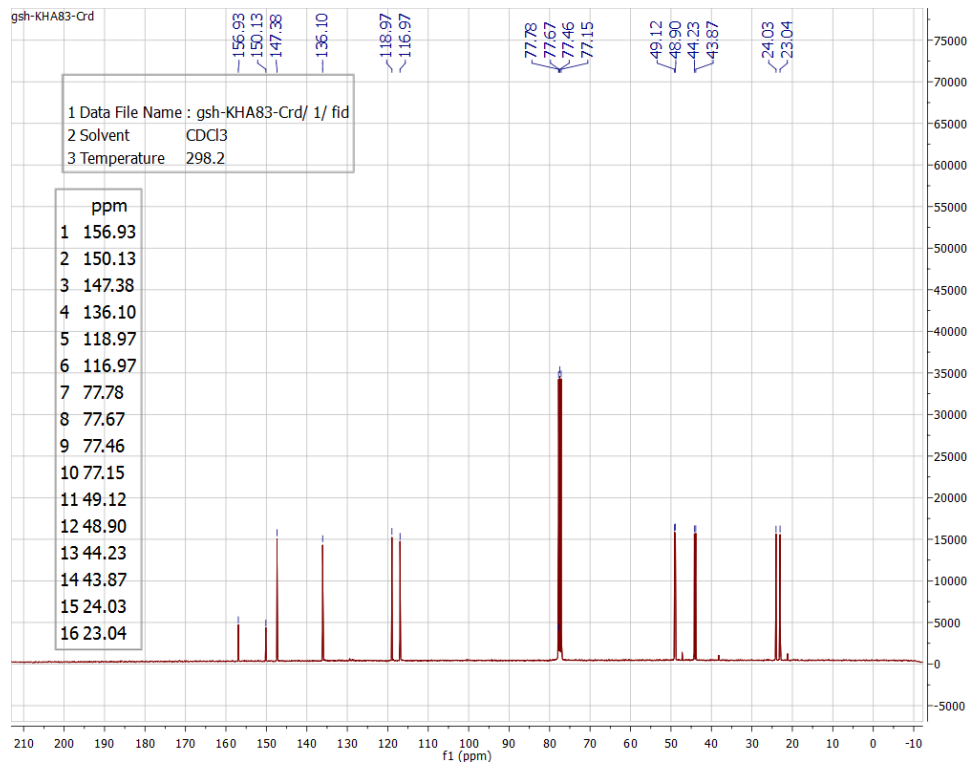


Figure S2. ^{13}C NMR spectrum of Guanidyl-pyridine, gpy in CDCl_3

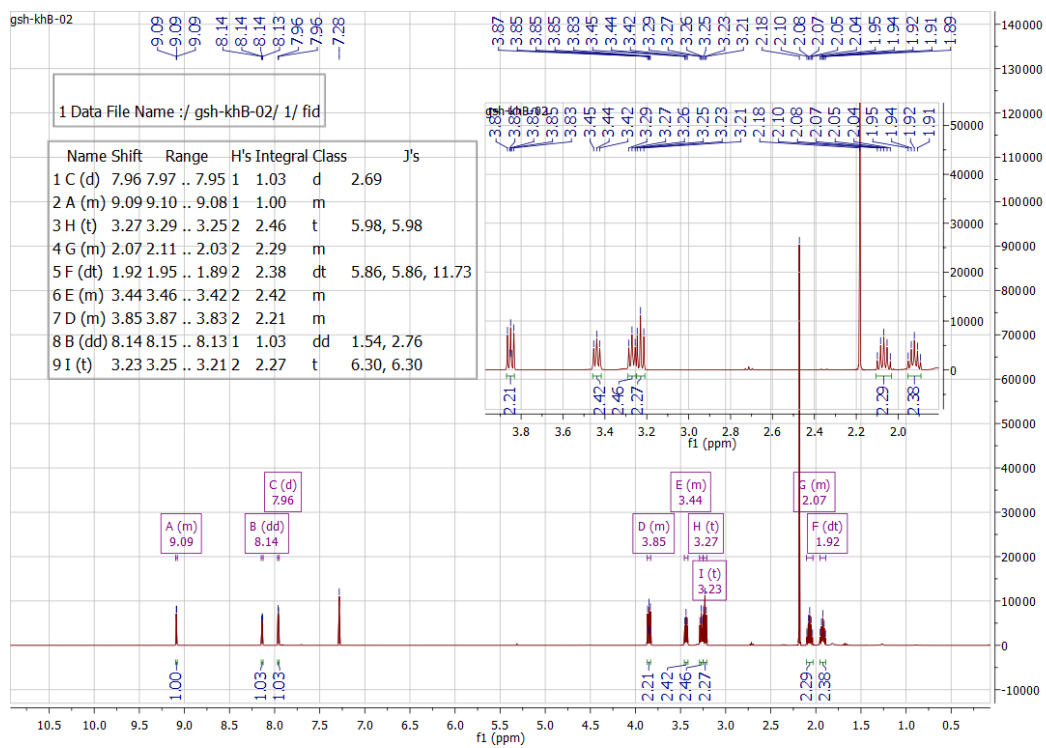


Figure S3. ^1H NMR spectrum of Guanidyl-pyrazine, gpz in CDCl_3

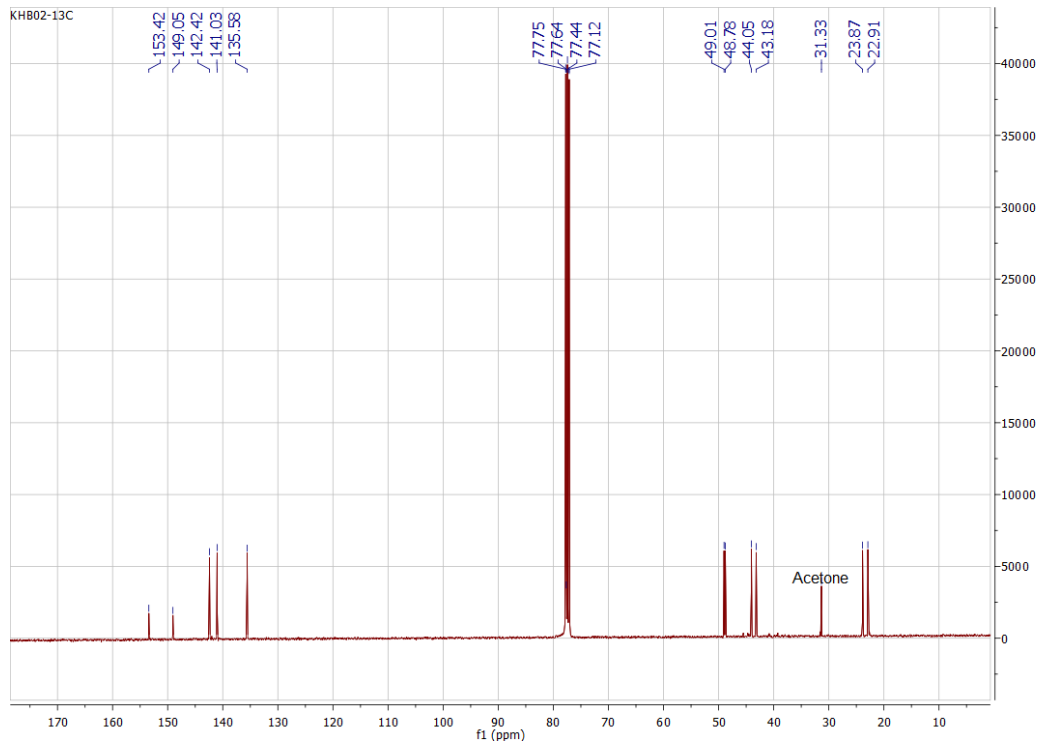


Figure S4. ^{13}C NMR spectrum of **Guanidyl-pyrazine, gpz** in CDCl_3

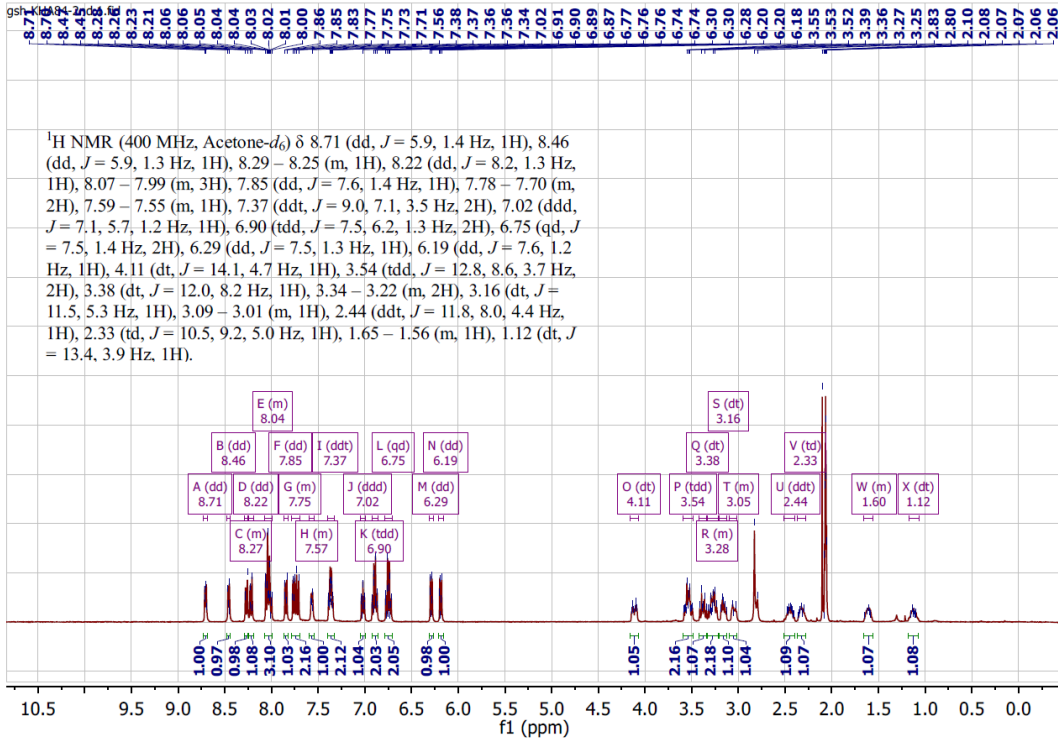


Figure S5. ^1H NMR spectrum of $[(\text{ppy})_2\text{Ir}(\text{gpy})]\text{PF}_6$, 1 in Acetone- d_6

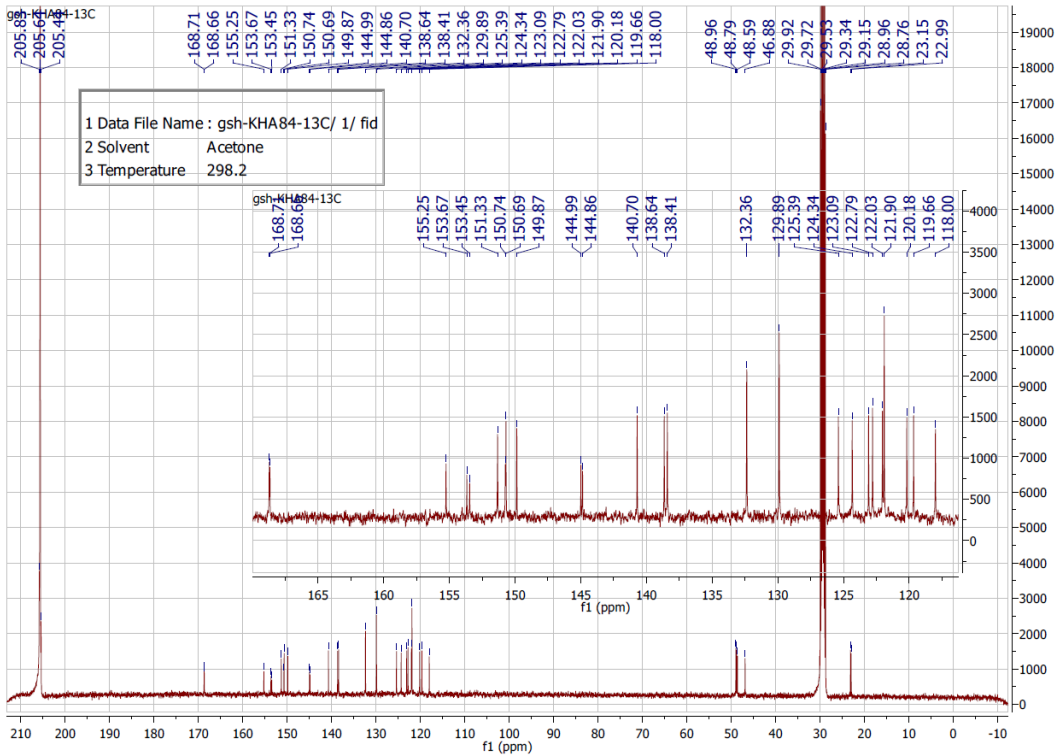


Figure S6. ^{13}C NMR spectrum of $[(\text{ppy})_2\text{Ir}(\text{gpy})]\text{PF}_6$, 1 in Acetone- d_6

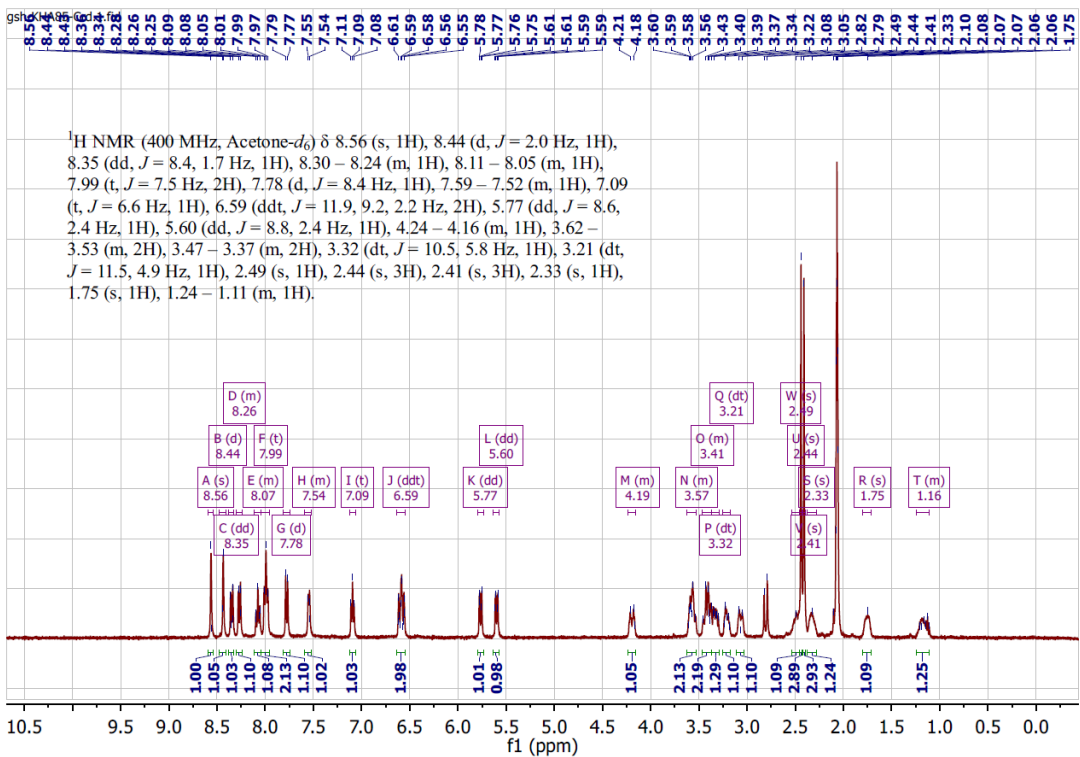


Figure S7. ¹H NMR spectrum of [(dFMeppy)₂Ir(gpy)]PF₆, 2 in Acetone-*d*₆

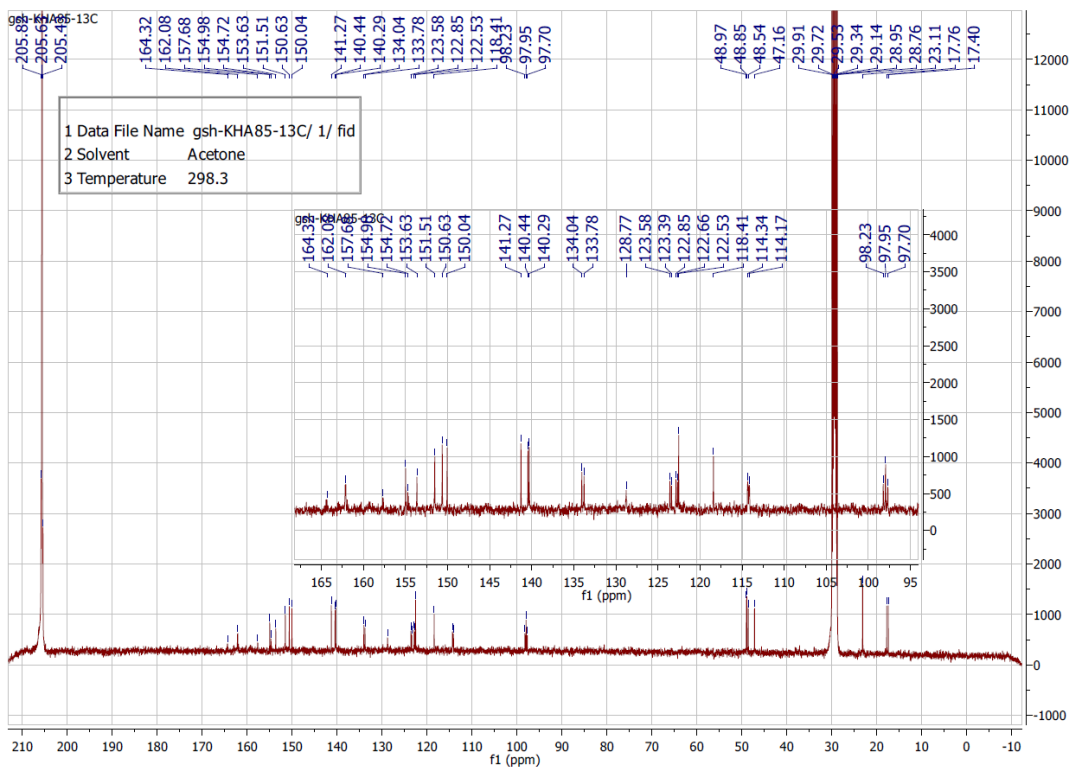


Figure S8. ¹³C NMR spectrum of [(dFMeppy)₂Ir(gpy)]PF₆, 2 in Acetone-*d*₆

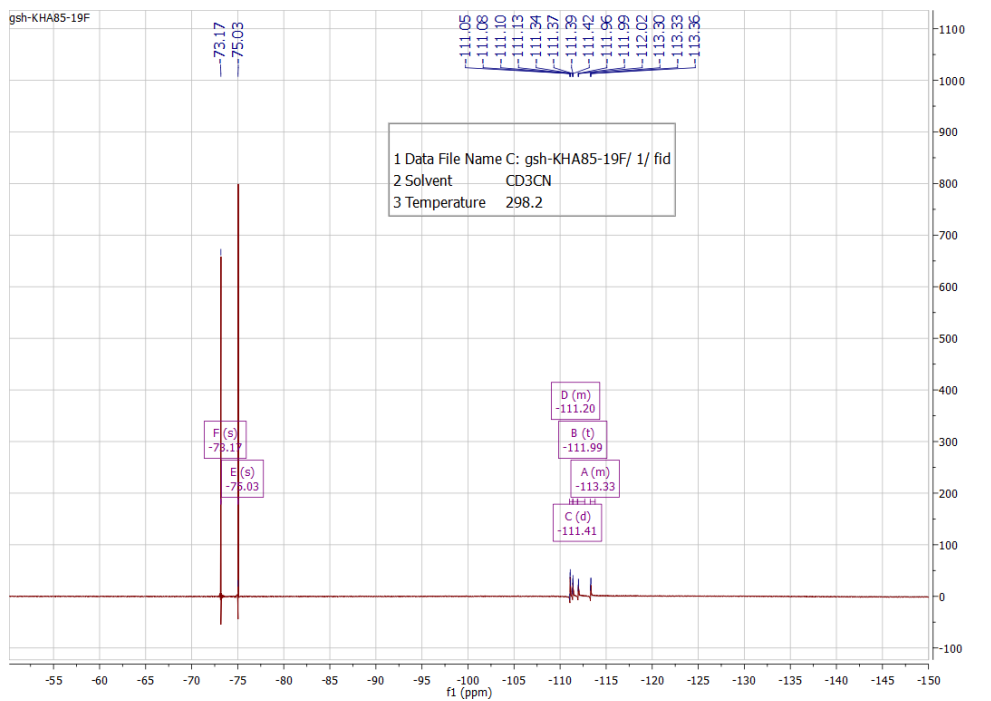


Figure S9. ^{19}F NMR spectrum of $[(\text{dFMeppy})_2\text{Ir}(\text{gpy})]\text{PF}_6$, **2** in Acetonitrile- d_3

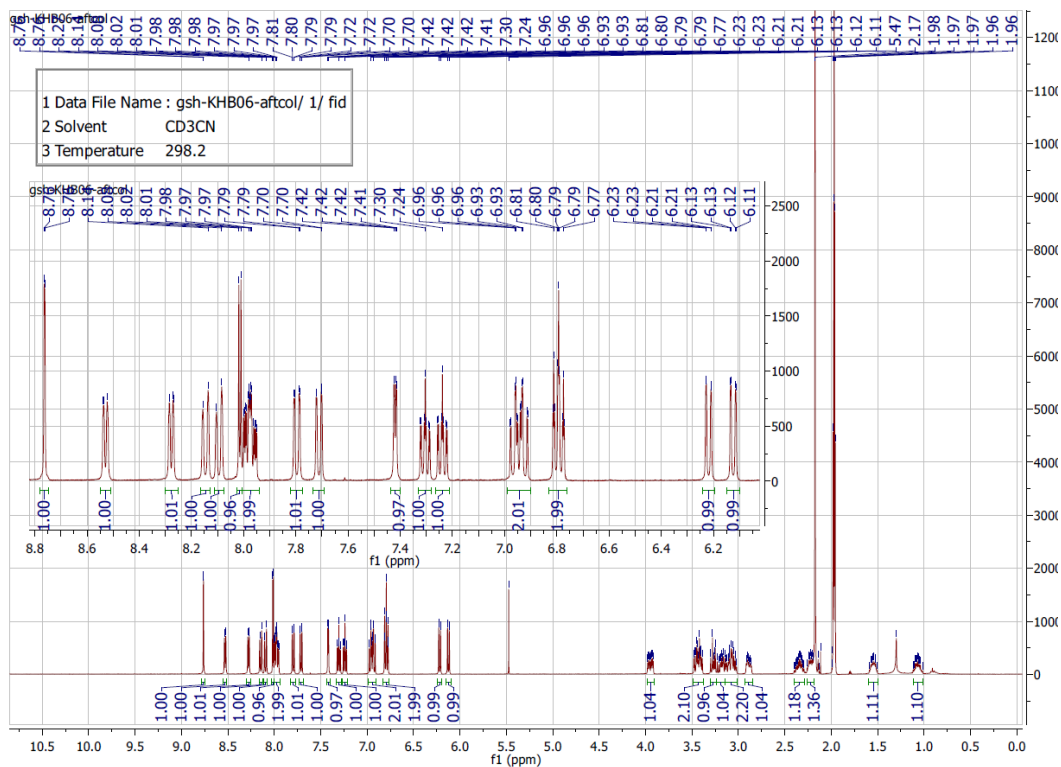


Figure S10. ^1H NMR spectrum of $[(\text{ppy})_2\text{Ir}(\text{gpz})]\text{PF}_6$, **3** in Acetonitrile- d_3

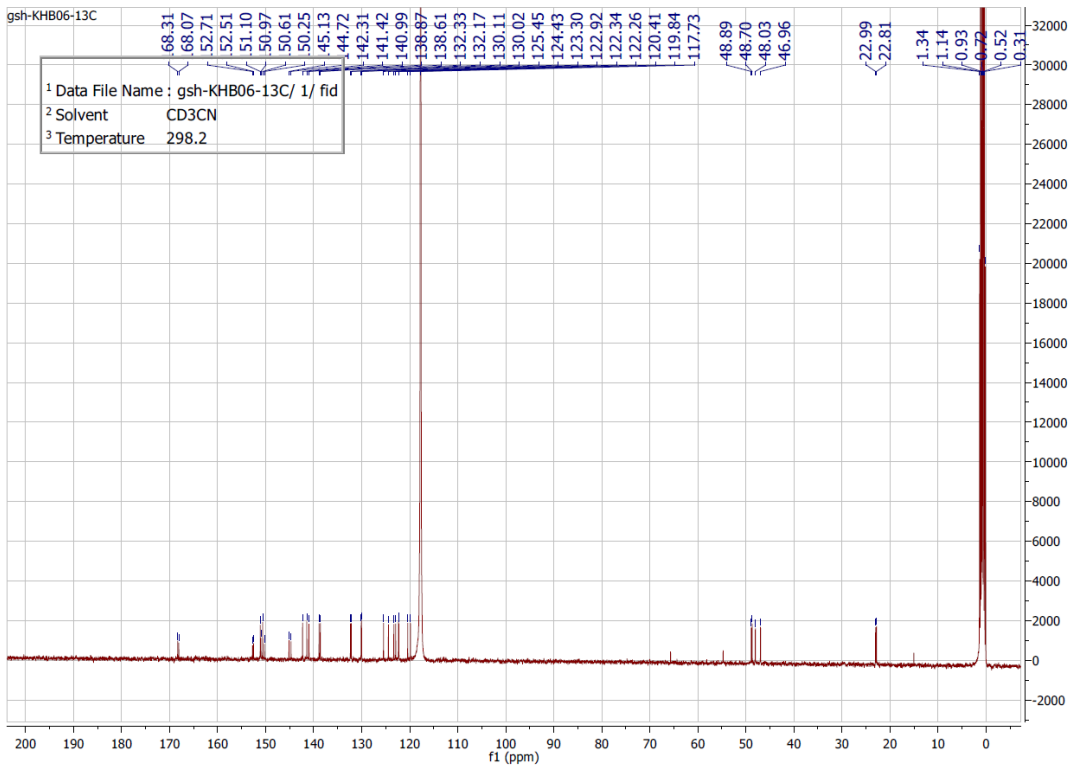


Figure S11. ^{13}C NMR spectrum of $[(\text{ppy})_2\text{Ir}(\text{gpz})]\text{PF}_6$, **3** in Acetonitrile- d_3

Crystallographic Section

X-ray crystallographic data were collected from a single crystal sample, which was mounted on a loop fiber. Data were collected using a Bruker Venture diffractometer equipped with a Photon 100 CMOS Detector, a Helios MX optics and a Kappa goniometer and a Gallium Liquid Metal Jet Source ($\lambda = 1.34139 \text{ \AA}$) at $100(2)$ K. The crystal-to-detector distance was 4.0 cm, and the data collection was carried out in 1024×1024 pixel mode. The initial unit cell parameters were determined by a least-squares fit of the angular setting of strong reflections, collected by a 110.0 degree scan in 110 frames over three different parts of the reciprocal space.

The diffraction quality of the best-available crystal was checked, revealing poor diffraction with a large amount of diffuse scattering. Data collection, cell refinement and data reduction were done using APEX2⁶ and SAINT.⁷ Absorption corrections were applied using SADABS.⁸

Structures were solved by direct methods using SHELXS2012 and refined on F^2 by full-matrix least squares using SHELXL2012.⁹ All non-hydrogen atoms were refined anisotropically. Hydrogen atoms were refined isotropic on calculated positions using a riding model. For compound **3** the highest difference peak is 3.23 Å far from Ir-atom and the deepest hole is 5.29 Å from H-atom. In addition, in **3** four more peaks with density around 2.88-1.81 e/Å³ were present essentially due to the quality of the crystal employed, which was the best available.

Table S1. Crystallographic data for complex **3**·CH₂Cl₂.

Compound	3 ·CH ₂ Cl ₂
CCDC Number	1015124
Formula	[C ₃₃ H ₃₁ N ₇ Ir][PF ₆]·CH ₂ Cl ₂
Mw (g/mol); d _{calcd.} (g/cm ³)	947.74; 1.830
T (K); F(000)	100(2); 3728
Crystal System	Orthorhombic
Space Group	Pbca
Unit Cell:	
a (Å)	10.9180(12)
b (Å)	16.0878(17)
c (Å)	39.160(4)
α (°)	90
β (°)	90
γ (°)	90
V (Å ³); Z	6878.4(13); 8
θ range (°); completeness	4.78-60.04; 0.991
R _{fle} :collec./indep.; R _{int}	110188/6939; 0.0740
μ (mm ⁻¹)	6.855
R1(F); wR(F ²); GoF(F ²) ^a	0.0787; 0.1875; 1.241
Residual electron density	3.23; -5.29

^aR1(F) based on observed reflections with I>2σ(I) for complex **3**; wR(F²) and GoF(F²) based on all data.

Table S2. Comparison of observed and calculated bond distances and angles of complex **3**.

Complex	Bond Length			Angle		
		Obs. (X-ray)	Calc. (DFT)		Obs. (X-ray)	Calc. (DFT)
3	Ir1-N1 _{ppy}	2.068(8)	2.08625	C1 _{ppy} -Ir1-N1 _{ppy}	80.6(4)	79.885
	Ir1-N2 _{ppy}	2.041(8)	2.08940	C12 _{ppy} -Ir1- N2 _{ppy}	80.8(4)	79.987
	Ir1-N3 _{gpz}	2.152(8)	2.23670	N3 _{gpz} -Ir1-N7 _{gpz}	83.8(3)	81.916
	Ir1-N7 _{gpz}	2.135(9)	2.24302			
	Ir1-C1 _{ppy}	1.998(11)	2.02302			
	Ir1-C12 _{ppy}	2.012(9)	2.02099			

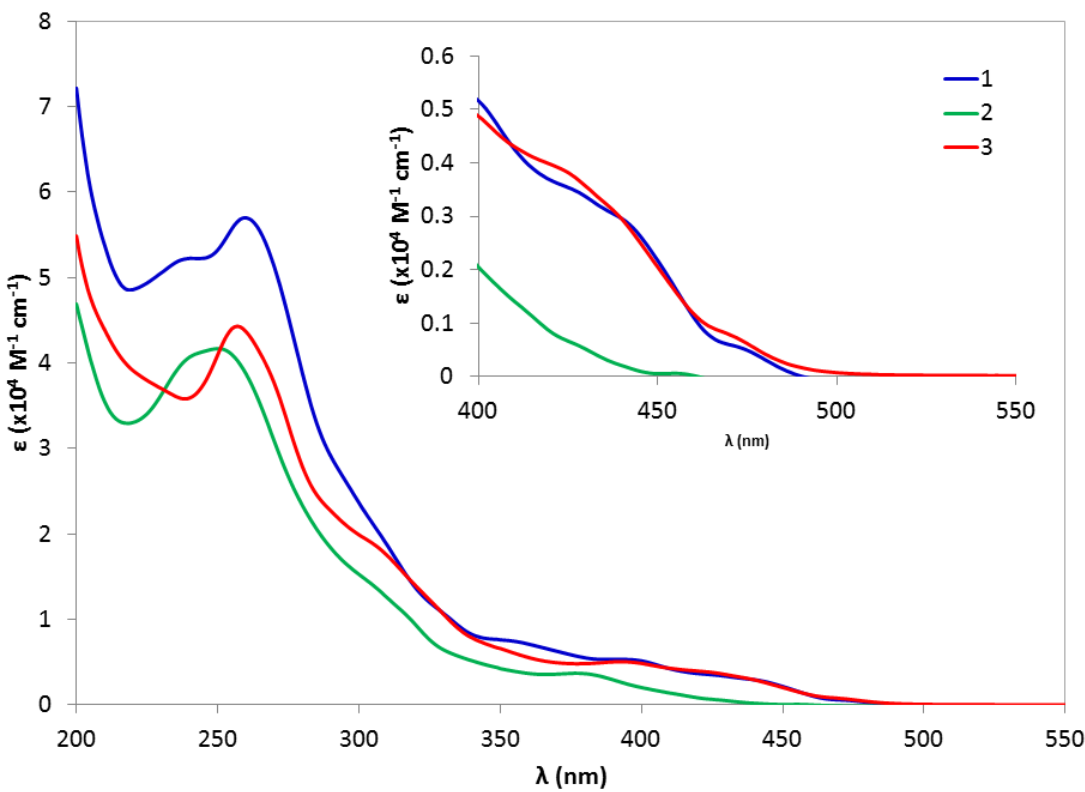


Figure S12. UV-vis absorption spectra of complexes **1-3** in acetonitrile at 298 K. Inset: Zoomed at lower energy transitions.

Table S3: Molar absorptivity data of complexes **1-3** in acetonitrile at 298 K.

Complex	$\lambda_{\text{abs}}/\text{nm} (\epsilon /10^4 \text{M}^{-1}\text{cm}^{-1})$	$E_{\text{HOMO}}/\text{eV}$ (TD-DFT)	$E_{\text{LUMO}}/\text{eV}$ (TD-DFT)	$ E_{\text{LUMO}} - E_{\text{HOMO}} /\text{eV}$ (conversion in nm in parenthesis) (TD-DFT)
1	241 (5.22); 260 (5.70); 360 (0.71); 403 (0.49); 445 (0.26); 477 (0.043)	-5.32	-1.6	3.72 (333 nm)
2	256 (4.06); 383 (2.16); 461 (0.003)	-5.66	-1.75	3.91 (317 nm)
3	257 (4.33); 311 (1.72); 402 (0.48); 443 (0.27); 477 (0.054)	-5.43	-2.12	3.31 (374 nm)

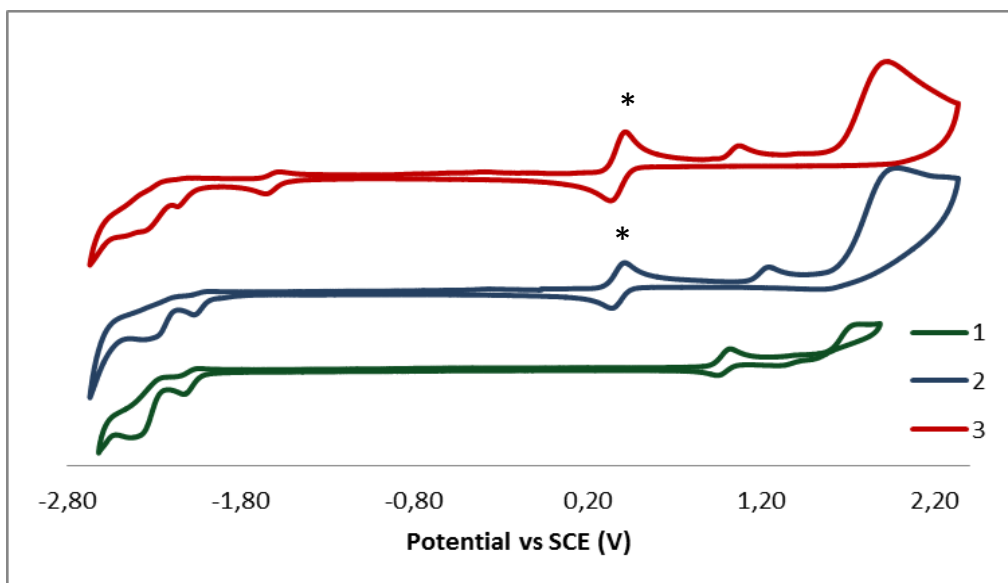


Figure S13. Cyclic voltammograms of complexes **1-3** in deaerated acetonitrile at 298 K using 0.1 M (*n*-Bu₄NPF₆) at the scan rate of 100 mV/s. The waves marked with an * correspond to the Fc+/Fc redox couple.

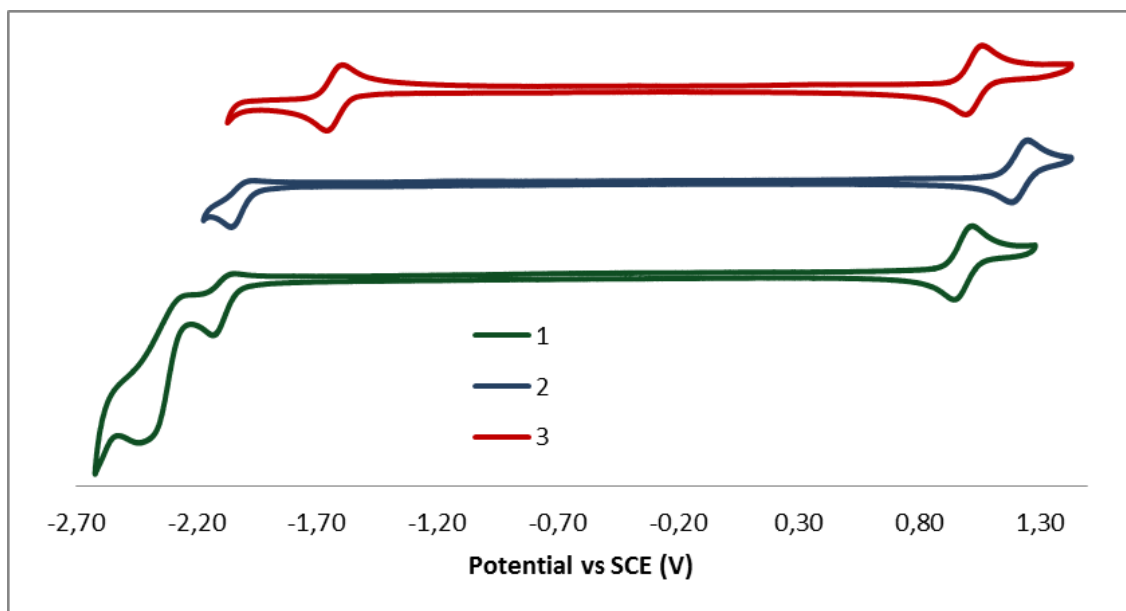


Figure S14. Cyclic voltammograms of complexes **1-3** up to 1st redox potential in deaerated acetonitrile at 298 K using 0.1 M (*n*-Bu₄NPF₆) at the scan rate of 100 mV/s.

Table S4: Electrochemical data of complexes **1-3** in degassed acetonitrile at 298 K.^a

Complex	$E_{1/2}^{\text{ox}}$ /V (ΔE_p)	$E_{\text{pa}}^{\text{ox}}$ / V	$E_{\text{pa}}^{\text{ox}}$ / V	$E_{1/2}^{\text{red}}$ /V (ΔE_p)	$E_{\text{pc}}^{\text{red}}$ / V	ΔE / V	E_{HOMO} /e V	E_{LUMO} /e V	$ E_{\text{LUMO}} - E_{\text{HOMO}} /\epsilon$ V
1	0.99 (88)	1.35	1.72	-2.13	-2.40	3.12	-5.32	-1.6	3.72
2	1.21 (72)	1.66	1.95	-2.12	-2.35	3.31	-5.66	-1.75	3.91
3	1.04 (82)	1.43	1.78	-1.60 (95)	-2.32 (131) ^b	2.72	-5.43	-2.12	3.31

^aCV traces recorded in ACN solution with 0.1 M (*n*-Bu₄N)PF₆ at 298 K at 50 mVs⁻¹. Values are in V vs. SCE (Fc/Fc⁺ vs. SCE = 0.38 V).¹⁹ $\Delta E = \Delta E_{\text{redox}}$; ΔE_p in mV = $|E_{\text{pa}} - E_{\text{pc}}|$, where E_{pa} = anodic peak potential and E_{pc} = cathodic peak potential; $E_{1/2} = (E_{\text{pa}} + E_{\text{pc}})/2$ and result from one-electron processes. A non-aqueous Ag/Ag⁺ electrode (silver wire in a solution of 0.1 M AgNO₃ in ACN) was used as the pseudoreference electrode; a glassy-carbon electrode was used for the working electrode and a Pt electrode was used as the counter electrode. E_{pa} reported for oxidation peak potentials and E_{pc} reported for reduction peak potentials. ^b $E_{1/2}^{\text{red}}$ for second reduction.

DFT Calculations:

Computational details:

All calculations were performed with the Gaussian03¹⁰ suite of programs employing the DFT method, the Becke three-parameter hybrid functional,¹¹ and Lee-Yang-Parr's gradient-corrected correlation functional (B3LYP).¹² Singlet ground state geometry optimizations for [1]¹⁺, [2]¹⁺ and [3]¹⁺ were carried out at the (R)B3LYP level in the gas phase, using the crystallographic structure of **3** as starting point. All elements except Ir were assigned to the 6-31G(d,p) basis set.¹³ The double- ζ quality LANL2DZ ECP basis set¹⁴ with an effective core potential and one additional f-type polarization was employed for the Ir-atom. Vertical electronic excitations based on (R)B3LYP-optimized geometries were computed for [1]¹⁺, [2]¹⁺ and [3]¹⁺ using the TD-DFT formalism^{15a,b} in acetonitrile using conductor-like polarizable continuum model (CPCM).^{16a-c} Vibrational frequency calculations were performed to ensure that the optimized geometries represent the local minima and there are only positive eigenvalues. The electronic distribution and localization of the singlet excited states were visualized using the electron density difference maps (ED-DMs).¹⁷ *Gausssum* 2.2 and *Chemissian* were employed to visualize the absorption spectra (simulated with Gaussian distribution with a full-width at half maximum (fwhm) set to 3000 cm⁻¹) and to calculate the fractional contributions of various groups to each molecular orbital. All calculated Kohn-Sham orbitals were visualized with ChemCraft.¹⁸

Table S5. Selected transitions from TD-DFT calculations of $[1]^{1+}$ in the singlet ground state (b3lyp/LanL2DZ(f)[Ir]6-31G**[C,H,N], CPCM (CH_3CN)).

Energy (eV)	λ/nm	$\lambda/\text{nm} (\epsilon \times 10^4 \text{ M}^{-1}\text{cm}^{-1})$ [expt.]	Oscillator strength	Major transition(s)	Character
5.04	246	241 (5.22)	0.211	H->L+7 (19%), H->L+8 (47%)	[ppy(π) to gpy(π^*) + ppy(π) to ppy(π^*)] (major) + [Ir(d π) to ppy(π^*) and gpy(π^*)] (minor)
4.77	260	260 (5.70)	0.224	H-6 -> L+2 (30%), H-2 -> L+5 (12%), H -> L+6 (12%)	[ppy(π) to gpy(π^*) + ppy(π) to ppy(π^*) + gpy(π) to gpy(π^*)] (major) + [Ir(d π) to ppy(π^*) and gpy(π^*)] (minor)
3.78	328	360 (0.71)	0.0787	H-3 -> L (33%), H-2 -> L (40%), H-1 -> L+1 (10%)	[ppy(π) to ppy(π^*)] (major) + [Ir(d π) to ppy(π^*)] (minor)
2.97	417	403 (0.49)	0.0455	H -> L (93%)	[ppy(π) to ppy(π^*)] (major) + [Ir(d π) to ppy(π^*)] (minor)

Table S6. Selected transitions from TD-DFT calculations of $[2]^{1+}$ in the singlet ground state (b3lyp/LanL2DZ(f)[Ir]6-31G**[C,H,N,F], CPCM (CH_3CN)).

Energy (eV)	λ/nm	$\lambda/\text{nm} (\epsilon \times 10^4 \text{ M}^{-1}\text{cm}^{-1})$ [expt.]	Oscillator strength	Major transition(s)	Character
4.79	259	256 (4.06)	0.217	H-2 -> L+4 (32%)	[dFMeppy(π) to dFMeppy(π^*)] (major) + [dFMeppy (π) to gpy(π^*) + gpy(n/ π) to gpy(π^*) + gpy(n/ π) to dFMeppy (π^*)] (minor)
3.15	394	383 (2.16)	0.040	H -> L (93%)	[dFMeppy (π) to dFMeppy (π^*) + Ir(d π) to dFMeppy (π^*)] (major) + [gpy(n/ π) to dFMeppy (π^*)] (minor)

Table S7. Selected transitions from TD-DFT calculations of [3]¹⁺ in the singlet ground state (b3lyp/LanL2DZ(f)[Ir]6-31G**[C,H,N], CPCM (CH₃CN)).

Energy (eV)	λ/nm	$\lambda/\text{nm} (\epsilon \times 10^4 \text{ M}^{-1}\text{cm}^{-1})$ [expt.]	Oscillator strength	Major transition(s)	Character
4.75	261	257 (4.33)	0.171	H-3 \rightarrow L+5 (16%), H-2 \rightarrow L+5 (23%)	[ppy(π) to ppy(π^*)] (major) + [Ir(d π) to ppy(π^*)] (minor)
3.85	322	311 (1.72)	0.074	H-3 \rightarrow L+1 (33%), H-2 \rightarrow L+1 (43%)	[ppy(π) to ppy(π^*)] (major) + [Ir(d π) to ppy(π^*)] (minor)
3.02	410	402 (0.48)	0.048	H \rightarrow L+1 (94%)	[ppy(π) to ppy(π^*)] + [Ir(d π) to ppy(π^*)] (almost equal contributions)
2.60	476	443 (0.27)	0.005	H \rightarrow L (98%)	[ppy(π) to gpz(π^*)] + [Ir(d π) to gpz(π^*)] (almost equal contributions)

Table S8. MO composition of [1]¹⁺ in Singlet ($S=0$) Ground State (b3lyp/LanL2DZ(f)[Ir]6-31G**[C,H,N]).

MO	Energy (eV)	Composition		
		Ir	ppy	gpy
LUMO+5	-0.79	2	28	71
LUMO+4	-0.96	1	78	21
LUMO+3	-1.04	3	88	10
LUMO+2	-1.36	2	8	90
LUMO+1	-1.52	4	90	7
LUMO	-1.6	4	95	1
HOMO	-5.32	42	47	11
HOMO-1	-5.94	44	25	31
HOMO-2	-6.09	14	80	6
HOMO-3	-6.2	43	50	7
HOMO-4	-6.42	18	76	6
HOMO-5	-6.52	2	94	5

Table S9. MO composition of $[2]^{1+}$ in Singlet ($S=0$) Ground State (b3lyp/LanL2DZ(f)[Ir]6-31G**[C,H,N,F]).

MO	Energy (eV)	Composition		
		Ir	dFMeppy	gpy
LUMO+5	-0.86	2	37	61
LUMO+4	-1.02	1	74	26
LUMO+3	-1.09	2	85	13
LUMO+2	-1.47	2	5	93
LUMO+1	-1.68	4	93	3
LUMO	-1.75	4	95	1
HOMO	-5.66	40	43	18
HOMO-1	-6.15	29	51	20
HOMO-2	-6.29	6	76	18
HOMO-3	-6.35	28	67	5
HOMO-4	-6.57	45	39	16
HOMO-5	-6.77	2	95	3

Table S10. MO composition of $[3]^{1+}$ in Singlet ($S=0$) Ground State (b3lyp/LanL2DZ(f)[Ir]6-31G**[C,H,N]).

MO	Energy (eV)	Composition		
		Ir	ppy	gpz
LUMO+5	-0.94	2	88	10
LUMO+4	-1.07	2	91	7
LUMO+3	-1.22	0	17	83
LUMO+2	-1.56	4	94	1
LUMO+1	-1.65	4	95	1
LUMO	-2.12	2	1	96
HOMO	-5.43	41	49	10
HOMO-1	-6.03	42	28	30
HOMO-2	-6.16	7	86	7
HOMO-3	-6.31	38	57	5
HOMO-4	-6.49	31	63	6
HOMO-5	-6.58	3	94	4

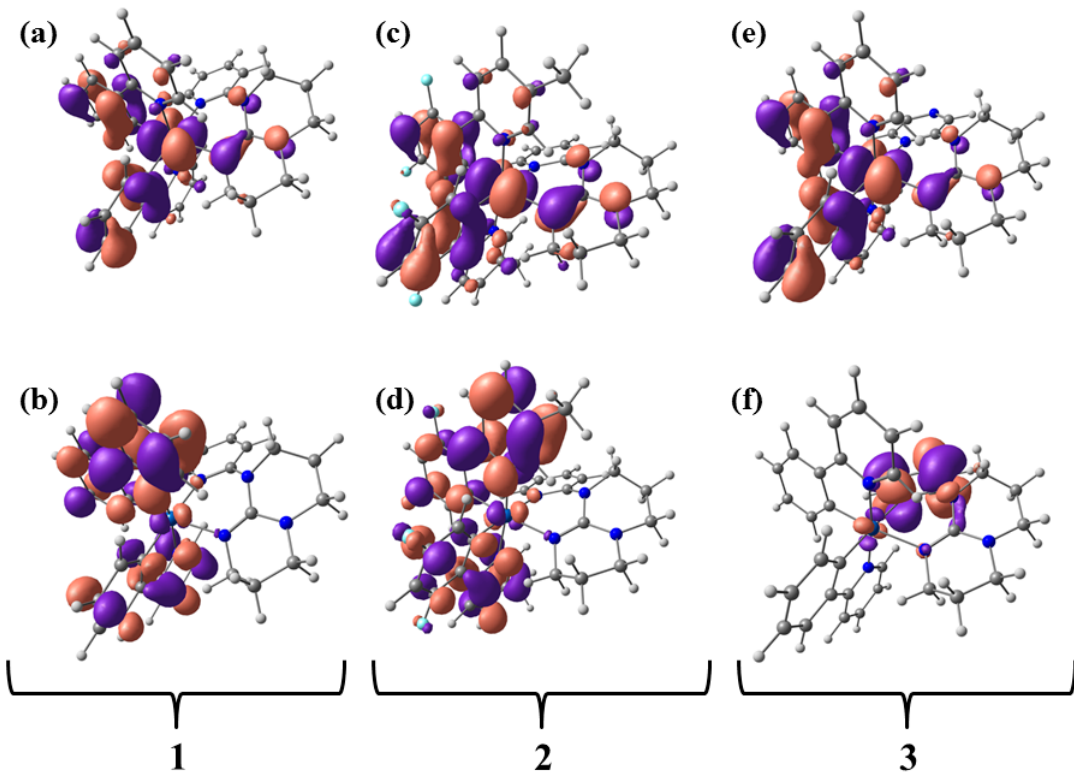


Figure S15: Kohn-Sham MO sketches of (a) HOMO and (b) LUMO of complex **1**, (c) HOMO and (d) LUMO of complex **2**, (e) HOMO and (f) LUMO of complex **3**.

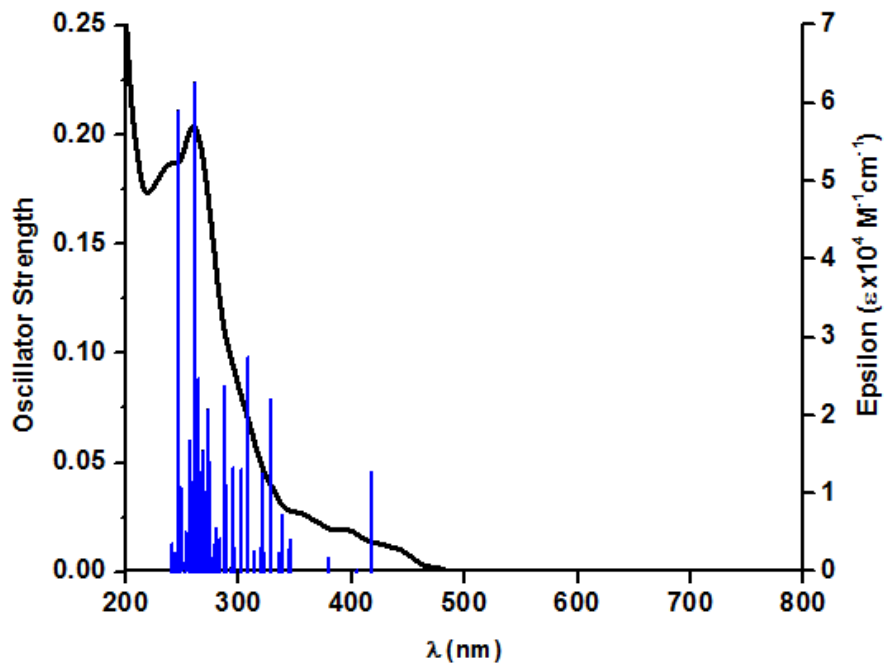


Figure S16. Overlay of experimental absorption spectra of the complex **1** in acetonitrile with its predicted transitions and oscillator strength, calculated by TD-DFT.

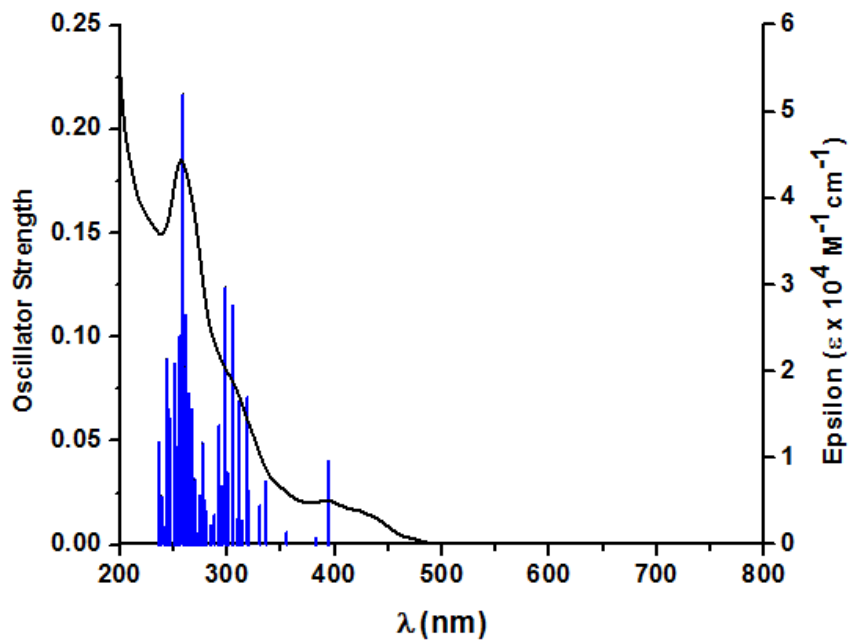


Figure S17. Overlay of experimental absorption spectra of the complex **2** in acetonitrile with its predicted transitions and oscillator strength, calculated by TD-DFT.

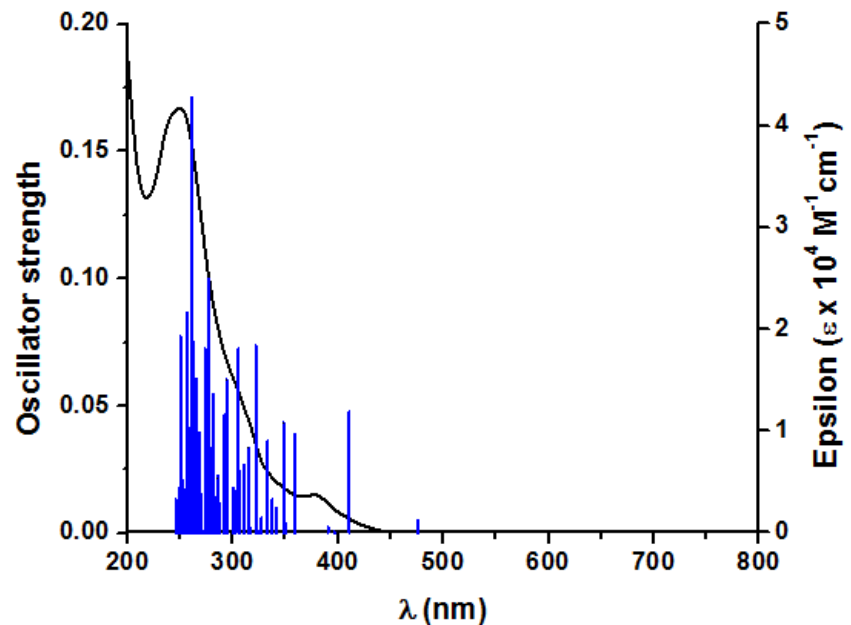


Figure S18. Overlay of experimental absorption spectra of the complex **3** in acetonitrile with its predicted transitions and oscillator strength, calculated by TD-DFT.

Table S11. Optimized atomic coordinates obtained from DFT calculations of **[1]¹⁺**

Center Number	Atomic Number	Atomic Type	Coordinates (Angstroms)		
			X	Y	Z
1	77	0	0.427957	0.020918	0.029433
2	7	0	1.243746	-1.357537	1.369877
3	7	0	-0.155222	1.420505	-1.403852
4	7	0	-0.974006	0.994594	1.493708
5	7	0	-2.906429	0.275958	0.275083
6	7	0	-1.299812	-1.383197	-0.194681
7	6	0	0.878532	-1.502827	2.659514
8	1	0	0.077560	-0.860335	3.001216
9	6	0	1.481998	-2.412285	3.513835
10	1	0	1.152653	-2.485623	4.543963
11	6	0	2.511927	-3.213883	3.012123
12	1	0	3.014925	-3.932689	3.651288
13	6	0	2.880045	-3.083313	1.681349
14	1	0	3.669240	-3.700935	1.270540
15	6	0	2.233327	-2.151770	0.853235
16	6	0	2.496744	-1.947357	-0.568821
17	6	0	3.441950	-2.695265	-1.293940
18	1	0	4.044763	-3.453725	-0.802931
19	6	0	3.614978	-2.469212	-2.653221
20	1	0	4.346036	-3.043405	-3.213300
21	6	0	2.840302	-1.493426	-3.290454
22	1	0	2.974149	-1.309778	-4.353283
23	6	0	1.902753	-0.747540	-2.573899
24	1	0	1.329982	0.009657	-3.099652
25	6	0	2.943735	1.394416	1.188602
26	1	0	3.140688	0.499796	1.771938
27	6	0	3.796135	2.491760	1.336464
28	1	0	4.633135	2.433660	2.027330
29	6	0	3.585338	3.661949	0.599861
30	1	0	4.248008	4.513202	0.718481
31	6	0	2.524616	3.721872	-0.296351
32	1	0	2.371179	4.628627	-0.874319
33	6	0	1.667841	2.618496	-0.449909
34	6	0	0.567155	2.582699	-1.409687
35	6	0	0.246366	3.595019	-2.328773
36	1	0	0.815926	4.516356	-2.325370
37	6	0	-0.773854	3.408943	-3.249206
38	1	0	-1.014602	4.189160	-3.964440

39	6	0	-1.471191	2.196424	-3.255278
40	1	0	-2.256078	1.994912	-3.975507
41	6	0	-1.128466	1.235149	-2.317232
42	1	0	-1.620807	0.272152	-2.285210
43	6	0	-0.441095	1.679292	2.532066
44	1	0	0.641421	1.731201	2.542894
45	6	0	-1.199123	2.302854	3.510021
46	1	0	-0.710595	2.851803	4.306717
47	6	0	-2.586783	2.191687	3.433185
48	1	0	-3.227055	2.637635	4.187732
49	6	0	-3.146159	1.484120	2.378650
50	1	0	-4.220060	1.366104	2.325076
51	6	0	-2.316920	0.906422	1.398601
52	6	0	-4.212695	0.777232	-0.189428
53	1	0	-4.175806	0.860241	-1.282226
54	1	0	-4.357274	1.783824	0.199682
55	6	0	-5.308298	-0.193223	0.234501
56	1	0	-5.309497	-0.297365	1.324057
57	1	0	-6.299388	0.162185	-0.062363
58	6	0	-5.018071	-1.532449	-0.439284
59	1	0	-5.432712	-2.368303	0.139161
60	1	0	-5.500844	-1.559697	-1.424617
61	6	0	-2.550222	-1.005342	-0.184599
62	7	0	-3.582869	-1.771290	-0.664198
63	6	0	-3.335972	-3.009050	-1.425855
64	1	0	-3.943257	-2.971006	-2.338997
65	1	0	-3.705770	-3.854360	-0.829907
66	6	0	-1.861230	-3.196629	-1.750071
67	1	0	-1.677449	-4.238445	-2.028367
68	1	0	-1.562817	-2.573032	-2.599780
69	6	0	-1.047418	-2.793553	-0.525237
70	1	0	0.017856	-2.913918	-0.710684
71	1	0	-1.311872	-3.430583	0.331202
72	6	0	1.702312	-0.951774	-1.199722
73	6	0	1.851074	1.430363	0.307590

Table S12. Optimized atomic coordinates obtained from DFT calculations of [2]¹⁺

Center Number	Atomic Number	Atomic Type	Coordinates (Angstroms)		
			X	Y	Z
1	77	0	-0.173675	-0.042646	-0.066024
2	7	0	-1.142935	-1.833257	-0.536058
3	7	0	0.557638	1.829178	0.497523
4	7	0	1.137915	0.023891	-1.876887
5	7	0	3.130738	-0.164000	-0.564656
6	7	0	1.500078	-1.286959	0.715915
7	6	0	-0.870860	-2.597583	-1.614118
8	1	0	-0.065597	-2.249437	-2.249072
9	6	0	-1.559424	-3.763213	-1.930610
10	6	0	-2.588644	-4.139263	-1.053988
11	1	0	-3.169013	-5.036571	-1.251130
12	6	0	-2.868633	-3.376633	0.067983
13	1	0	-3.654216	-3.668842	0.748328
14	6	0	-2.130178	-2.210034	0.334451
15	6	0	-2.279198	-1.324909	1.486698
16	6	0	-3.191514	-1.507971	2.539916
17	9	0	-4.045038	-2.557652	2.526364
18	6	0	-3.268515	-0.653984	3.626389
19	1	0	-3.983696	-0.820801	4.421637
20	6	0	-2.389287	0.424244	3.642200
21	9	0	-2.439161	1.270695	4.684483
22	6	0	-1.466690	0.661406	2.628552
23	1	0	-0.830788	1.534077	2.713722
24	6	0	-2.709295	0.743890	-1.613341
25	1	0	-2.979893	-0.301145	-1.710837
26	6	0	-3.537452	1.694582	-2.204563
27	9	0	-4.623086	1.279934	-2.877972
28	6	0	-3.285339	3.060424	-2.134764
29	1	0	-3.937441	3.787227	-2.602046
30	6	0	-2.160756	3.455251	-1.428865
31	9	0	-1.918423	4.784289	-1.361170
32	6	0	-1.291571	2.545646	-0.805296
33	6	0	-0.127298	2.903072	0.000629
34	6	0	0.298914	4.201028	0.334513
35	1	0	-0.234416	5.050121	-0.065901
36	6	0	1.376294	4.383439	1.185557
37	1	0	1.690792	5.390724	1.445073
38	6	0	2.048416	3.277264	1.728780

39	6	0	1.591862	2.022744	1.341025
40	1	0	2.050582	1.120568	1.726424
41	6	0	0.548514	0.171289	-3.086261
42	1	0	-0.531511	0.254395	-3.064118
43	6	0	1.249150	0.239751	-4.279034
44	6	0	2.637404	0.119806	-4.229579
45	1	0	3.234140	0.142557	-5.135944
46	6	0	3.253583	-0.049158	-2.998102
47	1	0	4.326358	-0.176922	-2.953062
48	6	0	2.482447	-0.077691	-1.820374
49	6	0	4.496338	0.379988	-0.453389
50	1	0	4.565673	0.929417	0.492597
51	1	0	4.649174	1.104190	-1.252140
52	6	0	5.501323	-0.765228	-0.477729
53	1	0	5.396476	-1.330948	-1.408605
54	1	0	6.531310	-0.399905	-0.430394
55	6	0	5.212485	-1.652089	0.732267
56	1	0	5.516408	-2.690579	0.547565
57	1	0	5.795115	-1.300268	1.593002
58	6	0	2.760582	-1.070429	0.447174
59	7	0	3.798555	-1.633089	1.145316
60	6	0	3.571171	-2.386033	2.392145
61	1	0	4.281735	-2.018856	3.142999
62	1	0	3.818339	-3.439728	2.205023
63	6	0	2.136168	-2.258649	2.879748
64	1	0	1.927997	-3.042418	3.613788
65	1	0	1.974522	-1.294686	3.374240
66	6	0	1.210277	-2.365484	1.673248
67	1	0	0.168111	-2.280266	1.973071
68	1	0	1.336694	-3.341868	1.184030
69	6	0	-1.394285	-0.206779	1.533330
70	6	0	-1.568083	1.151285	-0.911665
71	6	0	3.197398	3.433107	2.691912
72	1	0	4.011578	4.017709	2.249827
73	1	0	2.881944	3.957812	3.600170
74	1	0	3.602649	2.463504	2.994878
75	6	0	-1.214535	-4.569964	-3.155808
76	1	0	-0.943237	-5.597195	-2.889704
77	1	0	-2.066491	-4.628641	-3.841799
78	1	0	-0.374873	-4.132098	-3.702125
79	1	0	0.717404	0.378143	-5.213237

Table S13. Optimized atomic coordinates obtained from DFT calculations of [3]¹⁺

Center Number	Atomic Number	Atomic Type	Coordinates (Angstroms)		
			X	Y	Z
1	77	0	0.428448	0.016672	0.029639
2	7	0	1.207289	-1.398527	1.354855
3	7	0	-0.111758	1.448571	-1.388208
4	7	0	-0.962720	0.990854	1.485128
5	7	0	-2.916024	0.309505	0.270653
6	7	0	-1.325585	-1.354209	-0.244587
7	6	0	0.827009	-1.558553	2.638478
8	1	0	0.031225	-0.910942	2.982960
9	6	0	1.408636	-2.489463	3.484530
10	1	0	1.067931	-2.573974	4.510062
11	6	0	2.432340	-3.297560	2.980228
12	1	0	2.918830	-4.033080	3.613061
13	6	0	2.815918	-3.151407	1.655418
14	1	0	3.601009	-3.773239	1.243157
15	6	0	2.191004	-2.197911	0.835661
16	6	0	2.473423	-1.973201	-0.579699
17	6	0	3.415745	-2.722320	-1.307077
18	1	0	4.001767	-3.497883	-0.822648
19	6	0	3.607746	-2.475241	-2.660254
20	1	0	4.336759	-3.050451	-3.221876
21	6	0	2.854861	-1.477583	-3.289234
22	1	0	3.003352	-1.277805	-4.347127
23	6	0	1.919986	-0.730218	-2.570333
24	1	0	1.364203	0.043946	-3.089302
25	6	0	2.946212	1.330932	1.251963
26	1	0	3.115728	0.426756	1.829014
27	6	0	3.815753	2.411040	1.427438
28	1	0	4.638163	2.330456	2.133288
29	6	0	3.640539	3.592121	0.699309
30	1	0	4.316346	4.429603	0.839379
31	6	0	2.597633	3.681639	-0.215317
32	1	0	2.471151	4.597472	-0.785311
33	6	0	1.723371	2.596351	-0.396379
34	6	0	0.636097	2.594178	-1.372379
35	6	0	0.348232	3.623104	-2.283706
36	1	0	0.937996	4.531410	-2.264468
37	6	0	-0.667111	3.470082	-3.215755
38	1	0	-0.883035	4.263288	-3.924551

39	6	0	-1.393228	2.274770	-3.241189
40	1	0	-2.176741	2.100492	-3.969924
41	6	0	-1.081520	1.295244	-2.311432
42	1	0	-1.595967	0.343288	-2.293028
43	6	0	-0.452370	1.674071	2.533306
44	1	0	0.628763	1.731339	2.586212
45	6	0	-1.266083	2.287426	3.474008
46	1	0	-0.838120	2.847284	4.300195
47	6	0	-3.103662	1.522617	2.383400
48	1	0	-4.184458	1.434022	2.352801
49	6	0	-2.304286	0.923913	1.381535
50	6	0	-4.226409	0.826994	-0.169576
51	1	0	-4.202950	0.919362	-1.261781
52	1	0	-4.357954	1.831351	0.230304
53	6	0	-5.321118	-0.139682	0.262827
54	1	0	-5.307576	-0.250508	1.351619
55	1	0	-6.313539	0.225333	-0.016881
56	6	0	-5.049979	-1.475993	-0.425536
57	1	0	-5.454714	-2.313658	0.156963
58	1	0	-5.552737	-1.496063	-1.400729
59	6	0	-2.573387	-0.970175	-0.211794
60	7	0	-3.620092	-1.719794	-0.683306
61	6	0	-3.394690	-2.953598	-1.458412
62	1	0	-4.022880	-2.906851	-2.356664
63	1	0	-3.752595	-3.802148	-0.859974
64	6	0	-1.928534	-3.140644	-1.818032
65	1	0	-1.754242	-4.178609	-2.115849
66	1	0	-1.647829	-2.505302	-2.665167
67	6	0	-1.085212	-2.760024	-0.606317
68	1	0	-0.024915	-2.878314	-0.819350
69	1	0	-1.330272	-3.410628	0.245455
70	6	0	1.701674	-0.955346	-1.202622
71	6	0	1.872251	1.396880	0.350649
72	7	0	-2.600860	2.198701	3.407707

References:

- 1 M. Nonoyama, *Bull. Chem. Soc. Jpn.* **1974**, *47*, 767.
- 2 Crosby, G. A.; Demas, J. N. *J. Phys. Chem.* **1971**, *75*, 991.
- 3 W. H. Melhuish, *J. Phys. Chem.*, **1961**, *65*, 229–235.
- 4 V. V. Pavlishchuk and A. W. Addison, *Inorg. Chim. Acta* **2000**, *298*, 97.
- 5 A. K. Pal, S. Nag, J. G. Ferreira, V. Brochery, G. L. Ganga, A. Santora, S. Serroni, S. Campagna and G. S. Hanan, *Inorg. Chem.*, **2014**, *53*, 1679-1689.
- 6 *APEX2 (2013); Bruker Molecular Analysis Research Tool.* Bruker AXS Inc., Madison, WI 53719-1173.
- 7 (a) SAINT (2013) V8.34A; Integration Software for Single Crystal Data. Bruker AXS Inc., Madison, WI 53719-1173. (b) SAINT (2013) V8.34A; Integration Software for Single Crystal Data. Bruker AXS Inc., Madison, WI 53719-1173.
- 8 Sheldrick, G. M. (1996). *SADABS*, Bruker Area Detector Absorption Corrections. Bruker AXS Inc., Madison, WI 53719-1173.
- 9 *SHELXTL (2012) version 6.14*; Bruker Analytical X-ray Systems Inc., Madison, WI 53719-1173.
- 10 M. J. Frisch, G. W. Trucks, H. B. Schlegel, G. E. Scuseria, M. A. Robb, J. R. Cheeseman, J. A. Montgomery, T. J. Vreven, K. N. Kudin, J. C. Burant, J. M. S. Millam, J. Tomasi, V. Barone, B. Mennucci, M. Cossi, G. Scalmani, N. Rega, G. A. Petersson, H. Nakatsuji, M. Hada, M. Ehara, K. Toyota, R. Fukuda, J. Hasegawa, M. Ishida, T. Nakajima, Y. Honda, O. Kitao, H. Nakai, M. Klene, X. Li, J. E. Knox, H. P. Hratchian, J. B. Cross, C. Adamo, J. Jaramillo, R. Gomperts, R. E. Startmann, O. Yazyev, A. J. Austin, R. Cammi, C. Pomelli, J. W. Ochterski, P. Y. Ayala, K. Morokuma, G. A. Voth, P. Salvador, J. J. Dannenberg, V. G. Zakrzewski, J. M. Dapprich, A. D. Daniels, M. C. Strain, O. Farkas, D. K. Malick, A. D. Rabuck, K. Raghavachari, J. B. Foresman, J. V. Ortiz, Q. Cui, A. G. Baboul, S. Clifford, J. B. Cioslowski, G. Liu, A. Liashenko, I. Piskorz, L. M. R. Komaromi, D. J. Fox, T. Keith, M. A. Al-Laham, C. Y. Peng, A. Manayakkara, M. Challacombe, P. M. W. Gill, B. G. Johnson, W.

- Chen, M. W. Wong, C. Gonzalez, J. A. Pople, *Gaussian 2003, Revision C.02; Gaussian Inc.:Pittsburgh PA*, **2003**.
- 11 A. D. Becke, *J. Chem. Phys.* **1993**, *98*, 5648.
 - 12 C. Lee, W. Yang, R. G. Parr, *Phys. Rev. B: Condens. Matter* **1988**, *37*, 785.
 - 13 A. D. McLean, G. S. Chandler, *J. Chem. Phys.* **1980**, *72*, 5639.
 - 14 P. J. Hay, W. R. Wadt, *J. Chem. Phys.* **1985**, *82*, 270.
 - 15 a) M. E. Casida, C. Jamorski, K. C. Casida, D. R. Salahub, *J. Chem. Phys.* **1998**, *108*, 4439;
b) R. E. Stratmann, G. E. Scuseria, M. J. J. Frisch, *Chem. Phys.* **1998**, *109*, 8218.
 - 16 a) M. Cossi, N. Rega, G. Scalmani, V. Barone, *J. Comput. Chem.* **2003**, *24*, 669; b) M. Cossi, V. Barone, *J. Chem. Phys.* **2001**, *115*, 4708; c) V. Barone, M. Cossi, *J. Phys. Chem. A* **1998**, *102*, 1995.
 - 17 W. R. Browne, N. M. O'Boyle, J. J. McGarvey, J. G. Vos, *Chem. Soc. Rev.* **2005**, *34*, 641.
 - 18 D. A. Zhurko, G. A. Zhurko, *ChemCraft 1.5*; Plimus: San Diego, CA. Available at <http://www.chemcraftprog.com>.
 - 19 V. V. Pavlishchuk and A. W. Addison, *Inorg. Chim. Acta*, **2000**, *298*, 97.